JACS
JOURNAL OF THE AMERICAN CHEMICAL SOCIETY
pubs.acs.org/JACS
Communication

Visible Light Generation of a Microsecond Long-Lived Potent Reducing Agent

Zijian Zhao, Fushuang Niu, Pengju Li, Hanqi Wang, Zhenghao Zhang, Gerald J. Meyer,* and Ke Hu*

Cite This: J. Am. Chem. Soc. 2022, 144, 7043−7047
Read Online
ACCESS | Metrics & More | Article Recommendations | Supporting Information

ABSTRACT: Photoexcitation of molecular radicals can produce strong reducing agents; however, the limited lifetimes of the doublet excited states preclude many applications. Herein, we propose and demonstrate a general strategy to translate a highly energetic electron from a doublet excited state to a ZrO_2 insulator, thereby increasing the lifetime by about 6 orders of magnitude while maintaining a reducing potential less than −2.4 V vs SCE. Specifically, red light excitation of a salicylic acid modified perylene diimide radical anion $PDI^{\bullet-}$ anchored to a ZrO_2 insulator yields a $ZrO_2(e^-)$|PDI charge separated state with an ∼10 μs lifetime in 23% yield. The $ZrO_2(e^-)$s were shown to drive $CO_2 \rightarrow CO$ reduction with a Re catalyst present in micromolar concentrations. More broadly, this strategy provides new opportunities to reduce important reagents and catalysts at low concentrations through diffusional electron transfer.

Molecular doublet excited states have been identified with extreme redox potentials, either more oxidizing than fluorine gas or more reducing than alkali metals,[1−4] that drive energy-demanding redox reactions such as dehalogenation,[1,2,5,6] Birch reduction,[7] and arene oxidation[8] under the mild experimental conditions of room temperature and visible light irradiation.[9−11] Perylene diimides are the most well studied among a handful of open shell doublet excited states.[1,7,12−16] Detailed spectroscopic and kinetic studies from Schanze's group demonstrated that $^2(PDI^{\bullet-})^*$ underwent efficient electron transfer to organic acceptors;[16] however, the Stern−Volmer constants were small requiring large submolar acceptor concentrations even when the reactions were highly exergonic. High concentrations were necessary because excited state relaxation of the very short-lived ∼160 ps $^2(PDI^{\bullet-})^*$ otherwise precluded diffusional encounters with the acceptors. For expensive acceptors, such as the CO_2 reduction catalyst $Re(bpy)(CO)_3Cl$ (bpy = 2,2′-bipyridine), or acceptors with limited solubility, high concentrations are simply impractical. Here we propose and demonstrate a strategy to photogenerate reductants that are both potent and long-lived reducing agents.

The strategy is to transfer an electron from $^2(PDI^{\bullet-})^*$ to an insulator with a conduction band edge proximate to $E^0(PDI^{0/\bullet-*})$. A ZrO_2 insulator was selected for these initial studies due to its high transparency in the visible region and negative conduction band edge that is known to be inaccessible to common molecular excited states, Scheme 1. Indeed, mesoporous thin films of ZrO_2 nanoparticles have previously been utilized as reference materials for dye-sensitization studies when characterization of excited states was desired without complications from interfacial electron transfer.[17,18] We discovered that visible light excitation of ZrO_2|$PDI^{\bullet-}$ yielded a charge separated state, denoted as $ZrO_2(e^-)$|PDI, that has a stellar long lifetime of over ten microseconds while still maintaining a reduction potential more negative than −2.4 V vs the saturated calomel electrode (SCE). The collective ownership of both a long lifetime and strong reducing power in $ZrO_2(e^-)$|PDI was shown to enable

Scheme 1. Strategy for Photogeneration of a Potent and Long-Lived $ZrO_2(e^-)$ Reductant through Reductive Quenching of PDI* Followed by Doublet Excited State Electron Transfer from $^2(PDI^{\bullet-})^*$ to the ZrO_2 Conduction Band (CB)

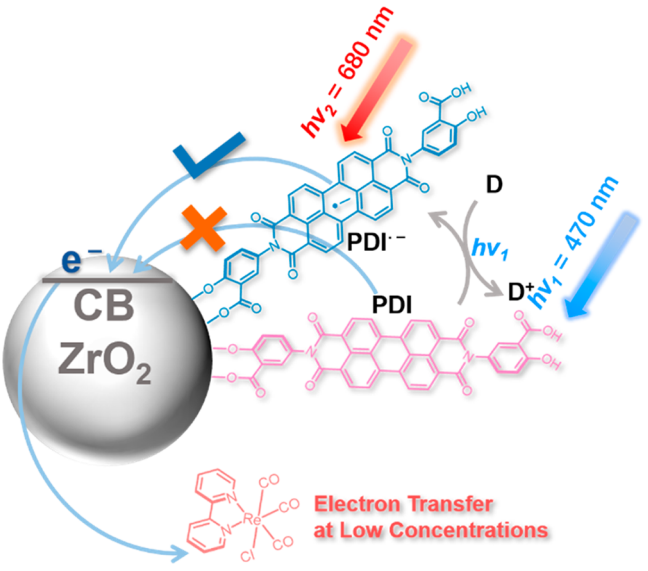

Received: January 12, 2022
Published: March 10, 2022

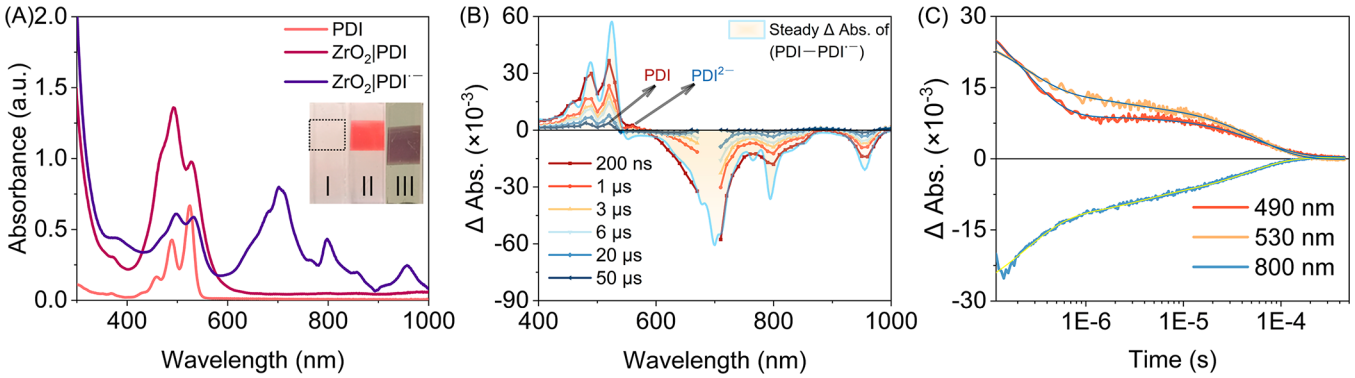

Figure 1. (A) The UV−vis−NIR absorption spectra of PDI, ZrO_2|PDI, and ZrO_2|$PDI^{\bullet-}$ in DMF. The inset shows pictures of unsensitized ZrO_2 film (I), ZrO_2|PDI (II), and ZrO_2|$PDI^{\bullet-}$ (III). (B) Absorption difference spectra of ZrO_2|$PDI^{\bullet-}$ after pulsed nanosecond laser excitation (λ_{ex} = 680 nm) at the indicated time delays. Overlaid in light blue is the absorption spectrum difference between PDI and $PDI^{\bullet-}$. (C) Representative absorbance changes monitored at 490, 530, and 800 nm after pulsed 680 nm excitation with overlaid fits to a triexponential kinetic model.

photocatalytic CO_2 reduction with a Re(bpy)$(CO)_3$Cl catalyst present in micromolar concentrations.

The photosensitizer *N*,*N*-Bis(3-carboxy-4-hydroxyphenyl)-perylene-3,4,9,10-bis(dicarboximide) (PDI) was synthesized by the reaction of 3,4,9,10-perylenetetracarboxydianhydride with 5-amino salicylic acid in hot imidazole, Scheme S1. The PDI was photoluminescent with a maximum at 527 nm and a lifetime of 3.8 ns in DMF. The PDI was anchored to the mesoporous ZrO_2 thin films by overnight reactions in a 2×10^{-4} M PDI DMF solution. Scanning electron microscopy studies of the resultant ZrO_2|PDI revealed a mesoporous thin film morphology of interconnected ∼10 nm ZrO_2 nanoparticles, Figure S2. Visible absorption spectroscopy quantified in a transmission mode was particularly useful for characterization of the ZrO_2|PDI redox chemistry. Representative comparative spectra acquired in DMF are shown in Figure 1A.

Relative to PDI dissolved in DMF, the spectrum of ZrO_2|PDI was broadened with a change in relative intensities attributed to intermolecular PDI−PDI interactions[19] and surface heterogeneity.[20] Chemical reduction of ZrO_2|PDI by tetrakis(dimethylamino)ethylene (TDAE) resulted in the appearance of new absorption features in the red and near-infrared regions with maintenance of an isosbestic point at 545 nm that were attributed to the formation of the reduced PDI, abbreviated as ZrO_2|$PDI^{\bullet-}$, Figure S3. Cyclic voltammetry studies of PDI in DMF electrolyte showed two reversible waves at −0.59 V and −0.81 V vs SCE that are given in Figure S4; however, the second reduction was not observed spectroscopically with excess TDAE. Photoreduction with white light excitation in the presence of triethanolamine (TEOA) as a sacrificial donor of ZrO_2|PDI revealed similar visible−NIR spectroscopic features as that measured by chemical reduction, Figure S5.

Visible light excitation of ZrO_2|PDI provided no evidence for interfacial electron transfer. Indeed, time-resolved photoluminescence (PL) decays of PDI and ZrO_2|PDI were within experimental error the same, 3.8 and 3.6 ns, respectively. Quenching was observed when PDI was anchored to TiO_2, Figure S6. The excited state reduction potential was calculated to be $E^0(PDI^{\bullet+/*}) = E^0(PDI^{\bullet+/0}) - E_{0-0} = -1.1$ V, where E_{0-0} was estimated from the intersection of the absorption and fluorescence spectra, Figure S7. This value is comparable to the conduction band edge of anatase TiO_2,[21] but is insufficient for ZrO_2. Capacitance measurements with Mott−Schottky analysis provided a preliminary estimate of the flat band potential at −2.4 V vs SCE with a more negative conduction band edge, Figure S8.

Figure 1B displays absorption difference spectra after pulsed 680 nm excitation of ZrO_2|$PDI^{\bullet-}$ measured at the indicated time delays. Overlaid in light blue is a simulated spectrum based on the absorption spectra of $PDI^{\bullet-}$ and PDI. The agreement between the simulated and measured spectra indicates that ZrO_2|$PDI^{\bullet-}$* injects an electron to ZrO_2 to form the charge separated state $ZrO_2(e^-)$|PDI. Comparative actinometry with a methylene blue actinometer provided a lower limit of 0.23 for the quantum yield for electron transfer from $^2(PDI^{\bullet-})$* to ZrO_2, Table S2. This yield is comparable to that previously reported for electron transfer from PDI* to TiO_2 for water oxidation applications, which indicates that electron transfer from a short-lived doublet excited state was as efficient as that for singlet excited state transfer across different metal oxide interfaces.[20]

The transient absorption features decreased cleanly to pre-excitation levels as the injected electron recombined with PDI. With one minor exception, the absorption data were fully consistent with quantitative $ZrO_2(e^-)$|PDI → ZrO_2|$PDI^{\bullet-}$ recombination. The minor exception was attributed to electron transfer from $ZrO_2(e^-)$ to $PDI^{\bullet-}$ to yield ZrO_2|PDI^{2-} with a characteristic absorption band at 560 nm, Figures S9 and S10. The yield of ZrO_2|PDI^{2-} was very small presumably because the insulating ZrO_2 prevents electron transport to distant $PDI^{\bullet-}$ acceptors.

The kinetics for interfacial $ZrO_2(e^-)$|PDI → ZrO_2|$PDI^{\bullet-}$ to yield the ground state were nonexponential, but were satisfactorily modeled by a triexponential function. An explanation for the nonexponential kinetics is lacking, yet such behavior is well documented in the dye sensitized TiO_2 literature.[22] Aggregation of PDI monomers and/or surface heterogeneity may also contribute to the kinetic behavior as indicated by the ground state absorption spectrum. Figure 1C shows representative kinetic data monitored at three wavelengths from which an average rate constant $\bar{k}_{cr} = 1.9 \pm 0.3 \times 10^4$ s^{-1} was extracted (shown in Table S1).

The remarkably long-lived $ZrO_2(e^-)$|PDI with reduction potential more negative than −2.4 V provides an opportunity for driving energy-demanding reactions with reactants or catalysts present in low micromolar concentrations. The classical CO_2 reduction catalyst *fac*-Re(bpy)$(CO)_3$Cl was chosen as a proof-of-principle example. Figure 2A displays transient absorption spectra measured after pulsed excitation of

https://doi.org/10.1021/jacs.2c00422
J. Am. Chem. Soc. 2022, 144, 7043−7047

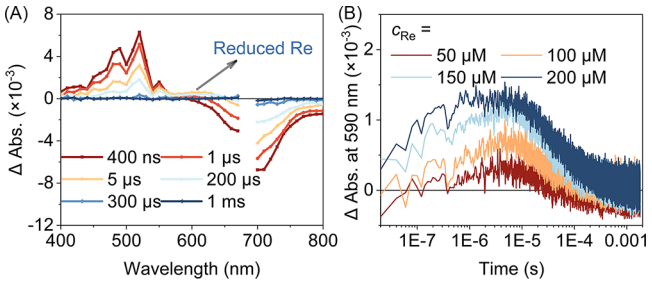

Figure 2. (A) Transient absorption spectra measured after pulsed 680 nm light excitation of ZrO_2|PDI$^{\bullet-}$ with 50 μM Re(bpy)(CO)$_3$Cl in DMF. (B) Absorbance change monitored at 590 nm at the indicated Re(bpy)(CO)$_3$Cl concentrations.

ZrO_2|PDI$^{\bullet-}$ in the presence of 50 μM Re(bpy)(CO)$_3$Cl in DMF. A notable new spectral feature appeared with a broad positive absorption band ~600 nm consistent with the formation of the reduced catalyst: [Re(bpy$^-$)(CO)$_3$Cl]$^-$.[23,24] In control experiments, this spectral feature was absent when Re(bpy)(CO)$_3$Cl was not present. Monitoring absorption changes at the 590 nm isosbestic point allowed the kinetics and yield of the reduced catalyst to be quantified without contributions from PDI redox chemistry. Figure 2B shows that the electron transfer rate and yield increased with the Re(bpy)(CO)$_3$Cl concentration from 50 to 200 μM.

Photocatalytic CO_2 reduction was carried out using ZrO_2|PDI, Re(bpy)(CO)$_3$Cl, and TEOA as the sacrificial electron donor in DMF under 100 mW/cm^2 LED white light illumination, Figure S11. Figure 3A shows the turnover number (TON) for CO_2 to CO catalysis measured over the course of 5 h. The TON of 34 is on par with that previously reported for photosensitized CO_2 catalysis.[25] Note that only trace H_2 was observed and the CO selectivity was over 99%. The catalytic TON were recovered when the ZrO_2|PDI was placed in a fresh DMF solution containing the same

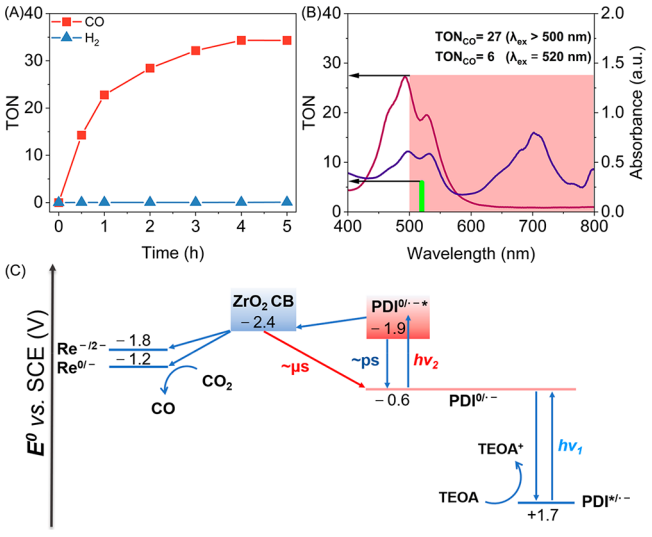

Figure 3. (A) TON of CO and H_2 by Re(bpy)(CO)$_3$Cl and ZrO_2|PDI as a function of irradiation time. (B) Photocatalytic CO_2 reduction TON under 520 nm irradiation or broad band irradiation with wavelengths greater than 500 nm. (C) Energetic and dynamic diagram of ZrO_2|PDI for CO_2 reduction upon visible light excitation. The Re catalyst reduction potentials were acquired from the literature.[24]

concentrations of Re(bpy)(CO)$_3$Cl and TEOA without a noticeable decrease in the TON over 5 repetitive cycles, Figure S12. The strong anchoring of salicylic acid to the ZrO_2 surface and efficient electron transfer at low catalyst concentrations renders the ZrO_2|PDI promising for catalysis applications.

Figure 3C shows an energy diagram for ZrO_2|PDI with the proposed photoinduced electron transfer processes for CO_2 reduction. The E^0(PDI$^{0/\bullet-}$) was measured by cyclic voltammetry with the previously reported excited state potential E^0(PDI$^{0/\bullet-*}$) = −1.9 V[16] indicate that injection into the ZrO_2 CB is thermodynamically uphill by about −0.5 eV. This suggests that electron transfer occurs from upper or "hot" excited state(s) and not the thermally equilibrated ^{2}(PDI$^{\bullet-}$)*. For example, the ^{2}(PDI$^{\bullet-}$) Franck−Condon excited state created upon absorption of a red 680 nm photon is a potent −2.4 V photoreductant that is thermodynamically competent of injection into ZrO_2. Hence, after light absorption excited state injection appears to occur in kinetic competition with relaxation to the thermally equilibrated excited state, behavior that is well documented in the dye-sensitized TiO_2 literature.[22]

The proposed mechanism involves the consecutive absorption of two photons, one by PDI to produce ^{2}(PDI$^{\bullet-}$) through reductive quenching of PDI*. The second photon is absorbed by ^{2}(PDI$^{\bullet-}$) to create the ^{2}(PDI$^{\bullet-}$)* excited state that injects an electron to form ZrO_2(e$^-$)|PDI. The injected electron then reduces the Re catalyst as the first elementary step in the catalytic cycle. To test this mechanism, wavelength-dependent photocatalytic CO_2 reduction experiments were performed, Figure 3B. With 520 nm light excitation (100 mW/cm^2), only limited catalytic performance (TON$_{CO}$ = 6) was observed over 4 h of illumination. In stark contrast, utilization of <100 mW/cm^2 from a white light source filtered to transmit wavelengths greater than 500 nm resulted in greatly improved TON$_{CO}$ of 27, behavior attributed to the significant long wavelength absorption by PDI$^{\bullet-}$. We therefore conclude that the second photon absorption by PDI$^{\bullet-}$ is critical to a high TON.

The ability of the ZrO_2|PDI photocatalyst to reduce aryl iodide and aryl chloride substrates with reduction potentials that ranged from −1.78 to −2.10 V was also investigated. Dehalogenation reactivity did indeed occur as is summarized in Scheme S2 with Figure S14−S16. In the case of 2-chloro-4-fluorobenzonitrile, nearly quantitative conversion to 4-fluorobenzonitrile was realized with an isolated yield of 86%. Collectively these data demonstrate that ZrO_2|PDI has significant promise for energy demanding photoredox catalysis applications.

Figure 4 summarizes the recent development of super-reductants based on their lifetimes and reduction potentials. With one exception,[26] a notable feature of this plot is that the most potent reductants have the shortest lifetimes. Significantly, this work revealed that a super-reductant based on molecule-insulator hybrid with a potential less than −2.0 V and a lifetime of ~10 μs can be generated with red light.

In conclusion, the strategy of utilizing a photochemically reduced insulator as a long-lived and potent reductant was realized. The ^{2}(PDI$^{\bullet-}$)* was shown to inject an electron into ZrO_2 to yield ZrO_2(e$^-$)|PDI with a quantum yield of 0.23 and a ~ ten microsecond long lifetime. The ZrO_2(e$^-$)|PDI was shown to activate CO_2 → CO catalysis and dehalogenate aryl halide even when the reactants were present in low micromolar concentrations. This interfacial electron transfer strategy differs

https://doi.org/10.1021/jacs.2c00422
J. Am. Chem. Soc. 2022, 144, 7043−7047

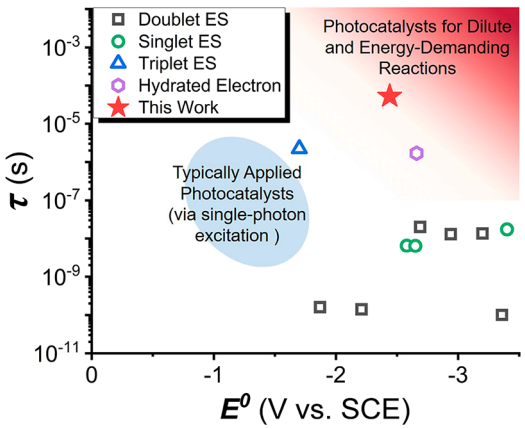

Figure 4. Previously reported reductants and $ZrO_2(e^-)$|PDI (red star) lifetime versus reduction potential.[2,11,16,19,26−31] ES is short for excited state.

significantly from the more traditional approach of synthesizing long-lived molecular excited states with larger energy gaps, minimal distortion (relative to the ground state), enhanced spin exchange, and/or greater charge delocalization.[32−36] While the search for long-lived reducing agents that can be generated with visible or near-infrared light is ongoing, this study demonstrates electron transfer to insulating materials as a new strategy for the realization of remarkably long-lived super-reductants.

■ ASSOCIATED CONTENT

Supporting Information

The Supporting Information is available free of charge at https://pubs.acs.org/doi/10.1021/jacs.2c00422.

Experimental details, additional spectroscopic and electrochemical characterizations, parallel photocatalytic CO_2 reduction runs, photocatalytic dehalogenation data, kinetic fitting, and injection yield calculations (PDF)

■ AUTHOR INFORMATION

Corresponding Authors

Gerald J. Meyer − *Department of Chemistry, University of North Carolina at Chapel Hill, Chapel Hill, North Carolina 27599-3290, United States;* orcid.org/0000-0002-4227-6393; Email: gjmeyer@email.unc.edu

Ke Hu − *Department of Chemistry and Shanghai Key Laboratory of Molecular Catalysis and Innovative Materials, Fudan University, Shanghai 200433, PR China;* orcid.org/0000-0002-0240-7192; Email: khu@fudan.edu.cn

Authors

Zijian Zhao − *Department of Chemistry and Shanghai Key Laboratory of Molecular Catalysis and Innovative Materials, Fudan University, Shanghai 200433, PR China*

Fushuang Niu − *Department of Chemistry and Shanghai Key Laboratory of Molecular Catalysis and Innovative Materials, Fudan University, Shanghai 200433, PR China*

Pengju Li − *Department of Chemistry and Shanghai Key Laboratory of Molecular Catalysis and Innovative Materials, Fudan University, Shanghai 200433, PR China*

Hanqi Wang − *Department of Chemistry and Shanghai Key Laboratory of Molecular Catalysis and Innovative Materials, Fudan University, Shanghai 200433, PR China*

Zhenghao Zhang − *Department of Chemistry and Shanghai Key Laboratory of Molecular Catalysis and Innovative Materials, Fudan University, Shanghai 200433, PR China*

Complete contact information is available at: https://pubs.acs.org/10.1021/jacs.2c00422

Notes

The authors declare no competing financial interest.

■ ACKNOWLEDGMENTS

This study is sponsored by the National Key R&D Program of China (2018YFE0201701) and the National Natural Science Foundation of China (21872037). The authors thank Dr. Menghui Jia at State Key Laboratory of Precision Spectroscopy, East China Normal University for helping with the fs-TA experiments. The authors also thank Dr. Renato N. Sampaio for his insightful comments and suggestions during the preparation of the manuscript.

■ REFERENCES

(1) Ghosh, I.; Ghosh, T.; Bardagi, J. I.; König, B. Reduction of aryl halides by consecutive visible light-induced electron transfer processes. *Science* **2014**, *346*, 725−728.

(2) MacKenzie, I. A.; Wang, L.; Onuska, N. P. R.; Williams, O. F.; Begam, K.; Moran, A. M.; Dunietz, B. D.; Nicewicz, D. A. Discovery and characterization of an acridine radical photoreductant. *Nature* **2020**, *580*, 76−80.

(3) Glaser, F.; Kerzig, C.; Wenger, O. S. Multi-Photon Excitation in Photoredox Catalysis: Concepts, Applications, Methods. *Angew. Chem., Int. Ed.* **2020**, *59*, 10266−10284.

(4) Wu, S.; Kaur, J.; Karl, T. A.; Tian, X.; Barham, J. P. Synthetic Molecular Photoelectrochemistry: New Frontiers in Synthetic Applications, Mechanistic Insights and Scalability. *Angew. Chem., Int. Ed.* **2022**, *61*, No. e202107811.

(5) Ghosh, I.; König, B. Chromoselective Photocatalysis: Controlled Bond Activation through Light-Color Regulation of Redox Potentials. *Angew. Chem., Int. Ed.* **2016**, *55*, 7676−7679.

(6) Graml, A.; Neveselý, T.; Jan Kutta, R.; Cibulka, R.; König, B. Deazaflavin reductive photocatalysis involves excited semiquinone radicals. *Nat. Commun.* **2020**, *11*, 3174−3184.

(7) Cole, J. P.; Chen, D. F.; Kudisch, M.; Pearson, R. M.; Lim, C. H.; Miyake, G. M. Organocatalyzed Birch Reduction Driven by Visible Light. *J. Am. Chem. Soc.* **2020**, *142*, 13573−13581.

(8) Targos, K.; Williams, O. P.; Wickens, Z. K. Unveiling Potent Photooxidation Behavior of Catalytic Photoreductants. *J. Am. Chem. Soc.* **2021**, *143*, 4125−4132.

(9) Chmiel, A. F.; Williams, O. P.; Chernowsky, C. P.; Yeung, C. S.; Wickens, Z. K. Non-innocent Radical Ion Intermediates in Photoredox Catalysis: Parallel Reduction Modes Enable Coupling of Diverse Aryl Chlorides. *J. Am. Chem. Soc.* **2021**, *143*, 10882−10889.

(10) Christensen, J. A.; Phelan, B. T.; Chaudhuri, S.; Acharya, A.; Batista, V. S.; Wasielewski, M. R. Phenothiazine Radical Cation Excited States as Super-oxidants for Energy-Demanding Reactions. *J. Am. Chem. Soc.* **2018**, *140*, 5290−5299.

(11) Xu, J.; Cao, J.; Wu, X.; Wang, H.; Yang, X.; Tang, X.; Toh, R. W.; Zhou, R.; Yeow, E. K. L.; Wu, J. Unveiling Extreme Photoreduction Potentials of Donor-Acceptor Cyanoarenes to Access Aryl Radicals from Aryl Chlorides. *J. Am. Chem. Soc.* **2021**, *143*, 13266−13273.

(12) Zeng, L.; Liu, T.; He, C.; Shi, D.; Zhang, F.; Duan, C. Organized Aggregation Makes Insoluble Perylene Diimide Efficient for the Reduction of Aryl Halides via Consecutive Visible Light-Induced Electron-Transfer Processes. *J. Am. Chem. Soc.* **2016**, *138*, 3958−61.

(13) Cybularczyk-Cecotka, M.; Szczepanik, J.; Giedyk, M. Photocatalytic strategies for the activation of organic chlorides. *Nat. Catal.* **2020**, *3*, 872−886.
(14) Chen, Y.-J.; Lei, T.; Hu, H.-L.; Wu, H.-L.; Zhou, S.; Li, X.-B.; Chen, B.; Tung, C.-H.; Wu, L.-Z. Tandem photoelectrochemical and photoredox catalysis for efficient and selective aryl halides functionalization by solar energy. *Matter* **2021**, *4*, 2354−2366.
(15) Cowper, N. G. W.; Chernowsky, C. P.; Williams, O. P.; Wickens, Z. K. Potent Reductants via Electron-Primed Photoredox Catalysis: Unlocking Aryl Chlorides for Radical Coupling. *J. Am. Chem. Soc.* **2020**, *142*, 2093−2099.
(16) Zeman, C. J.; Kim, S.; Zhang, F.; Schanze, K. S. Direct Observation of the Reduction of Aryl Halides by a Photoexcited Perylene Diimide Radical Anion. *J. Am. Chem. Soc.* **2020**, *142*, 2204−2207.
(17) Hanson, K.; Brennaman, M. K.; Ito, A.; Luo, H.; Song, W.; Parker, K. A.; Ghosh, R.; Norris, M. R.; Glasson, C. R. K.; Concepcion, J. J.; Lopez, R.; Meyer, T. J. Structure−Property Relationships in Phosphonate-Derivatized, RuII Polypyridyl Dyes on Metal Oxide Surfaces in an Aqueous Environment. *J. Phys. Chem. C* **2012**, *116*, 14837−14847.
(18) Bangle, R. E.; Mortelliti, M. J.; Troian-Gautier, L.; Dempsey, J. L.; Meyer, G. J. Tunneling and Thermally Activated Electron Transfer in Dye-Sensitized SnO_2|TiO_2 Core|Shell Nanostructures. *J. Phys. Chem. C* **2020**, *124*, 25148−25159.
(19) Li, H.; Wenger, O. S. Photophysics of Perylene Diimide Dianions and Their Application in Photoredox Catalysis. *Angew. Chem., Int. Ed.* **2022**, *61*, No. e202110491.
(20) Shan, B.; Nayak, A.; Brennaman, M. K.; Liu, M.; Marquard, S. L.; Eberhart, M. S.; Meyer, T. J. Controlling Vertical and Lateral Electron Migration Using a Bifunctional Chromophore Assembly in Dye-Sensitized Photoelectrosynthesis Cells. *J. Am. Chem. Soc.* **2018**, *140*, 6493−6500.
(21) Xu, Y.; Zheng, J.; Lindner, J. O.; Wen, X.; Jiang, N.; Hu, Z.; Liu, L.; Huang, F.; Würthner, F.; Xie, Z. Consecutive Charging of a Perylene Bisimide Dye by Multistep Low-Energy Solar-Light-Induced Electron Transfer Towards H_2 Evolution. *Angew. Chem., Int. Ed.* **2020**, *59*, 10363−10367.
(22) Ardo, S.; Meyer, G. J. Photodriven heterogeneous charge transfer with transition-metal compounds anchored to TiO_2 semiconductor surfaces. *Chem. Soc. Rev.* **2009**, *38*, 115−164.
(23) Li, T.-T.; Shan, B.; Meyer, T. J. Stable Molecular Photocathode for Solar-Driven CO_2 Reduction in Aqueous Solutions. *ACS Energy Lett.* **2019**, *4*, 629−636.
(24) Lee, Y. F.; Kirchhoff, J. R.; Berger, R. M.; Gosztola, D. Spectroelectrochemistry and excited-state absorption spectroscopy of rhenium(I)α,α'-diimine complexes. *J. Chem. Soc., Dalton Trans.* **1995**, 3677−3682.
(25) Cheung, P. L.; Kapper, S. C.; Zeng, T.; Thompson, M. E.; Kubiak, C. P. Improving Photocatalysis for the Reduction of CO_2 through Non-covalent Supramolecular Assembly. *J. Am. Chem. Soc.* **2019**, *141*, 14961−14965.
(26) Glaser, F.; Larsen, C. B.; Kerzig, C.; Wenger, O. S. Aryl dechlorination and defluorination with an organic super-photoreductant. *Photochem. Photobio. Sci.* **2020**, *19*, 1035−1041.
(27) Kerzig, C.; Wenger, O. S. Reactivity control of a photocatalytic system by changing the light intensity. *Chem. Sci.* **2019**, *10*, 11023−11029.
(28) La Porte, N. T.; Martinez, J. F.; Hedstrom, S.; Rudshteyn, B.; Phelan, B. T.; Mauck, C. M.; Young, R. M.; Batista, V. S.; Wasielewski, M. R. Photoinduced electron transfer from rylenediimide radical anions and dianions to $Re(bpy)(CO)_3$ using red and near-infrared light. *Chem. Sci.* **2017**, *8*, 3821−3831.
(29) Connell, T. U.; Fraser, C. L.; Czyz, M. L.; Smith, Z. M.; Hayne, D. J.; Doeven, E. H.; Agugiaro, J.; Wilson, D. J. D.; Adcock, J. L.; Scully, A. D.; Gomez, D. E.; Barnett, N. W.; Polyzos, A.; Francis, P. S. The Tandem Photoredox Catalysis Mechanism of $[Ir(ppy)_2(dtb\text{-}bpy)](+)$ Enabling Access to Energy Demanding Organic Substrates. *J. Am. Chem. Soc.* **2019**, *141*, 17646−17658.
(30) Kim, H.; Kim, H.; Lambert, T. H.; Lin, S. Reductive Electrophotocatalysis: Merging Electricity and Light To Achieve Extreme Reduction Potentials. *J. Am. Chem. Soc.* **2020**, *142*, 2087−2092.
(31) Rieth, A. J.; Gonzalez, M. I.; Kudisch, B.; Nava, M.; Nocera, D. G. How Radical Are "Radical" Photocatalysts? A Closed-Shell Meisenheimer Complex Is Identified as a Super-Reducing Photoreagent. *J. Am. Chem. Soc.* **2021**, *143*, 14352−14359.
(32) Treadway, J. A.; Strouse, G. F.; Ruminski, R. R.; Meyer, T. J. Long-Lived Near-Infrared MLCT Emitters. *Inorg. Chem.* **2001**, *40*, 4508−4509.
(33) Zhao, X.; Yao, Q.; Long, S.; Chi, W.; Yang, Y.; Tan, D.; Liu, X.; Huang, H.; Sun, W.; Du, J.; Fan, J.; Peng, X. An Approach to Developing Cyanines with Simultaneous Intersystem Crossing Enhancement and Excited-State Lifetime Elongation for Photodynamic Antitumor Metastasis. *J. Am. Chem. Soc.* **2021**, *143*, 12345−12354.
(34) Medlycott, E. A.; Hanan, G. S. Synthesis and properties of mono- and oligo-nuclear Ru(II) complexes of tridentate ligands: The quest for long-lived excited states at room temperature. *Coord. Chem. Rev.* **2006**, *250*, 1763−1782.
(35) Ren, Y.; Lam, J. W. Y.; Dong, Y.; Tang, B. Z.; Wong, K. S. Enhanced Emission Efficiency and Excited State Lifetime Due to Restricted Intramolecular Motion in Silole Aggregates. *J. Phys. Chem. B* **2005**, *109*, 1135−1140.
(36) Garakyaraghi, S.; McCusker, C. E.; Khan, S.; Koutnik, P.; Bui, A. T.; Castellano, F. N. Enhancing the Visible-Light Absorption and Excited-State Properties of Cu(I) MLCT Excited States. *Inorg. Chem.* **2018**, *57*, 2296−2307.

https://doi.org/10.1021/jacs.2c00422
J. Am. Chem. Soc. 2022, 144, 7043−7047